

A generalized Bellman-Ford Algorithm for Application in Symbolic Optimal Control

Alexander Weber, Marcus Kreuzer and Alexander Knoll

Abstract—Symbolic controller synthesis is a fully-automated and correct-by-design synthesis scheme whose limitations are its immense memory and runtime requirements. A current trend to compensate for this downside is to develop techniques for parallel execution of the scheme both in mathematical foundation and in software implementation. In this paper we present a generalized Bellman-Ford algorithm to be used in the so-called symbolic optimal control, which is an extension of the aforementioned synthesis scheme. Compared to the widely used Dijkstra algorithm our algorithm has two advantages. It allows for cost functions taking arbitrary (e.g. negative) values and for parallel execution with the ability for trading processing speed for memory consumption. We motivate the usefulness of negative cost values on a scenario of aerial firefighting with unmanned aerial vehicles. In addition, this four-dimensional numerical example, which is rich in detail, demonstrates the great performance of our algorithm.

I. INTRODUCTION

Symbolic controller synthesis is attracting considerable attention in the last two decades, see [1]–[4] and the many references in these works. This synthesis scheme takes a plant and a control specification formulation as input and attempts to solve the resulting control problem algorithmically without an intermediate intervention of the engineer. In case the process terminates successfully, a controller is returned possessing the formal guarantee that the resulting closed loop meets the given specification. A subsequent verification routine is not required. Processable plants are sampled-data control systems whose underlying continuous-time dynamics are given by nonlinear differential equations/inclusions. Specifications can be in principle quite arbitrary. However, efficient algorithms have been presented only for safety, reach-avoid [5] and GR(1)-specifications [6]. (Applications of these algorithms in symbolic control can be also found in [2], [7], [8].) In addition, the basic theory has been recently extended to optimal control problems so that near-optimal controllers with respect to a given non-negative cost function can be synthesized [9], [10].

Though making most of the empirical synthesis techniques obsolete in principle, symbolic controller synthesis has not become a standard technique until now. The main problem is the “curse of dimensionality”, from which this approach suffers. I.e. memory consumption and runtime are growing exponentially with increasing state space dimension of the given plant. The runtime is due to, among other things, the solution of initial value problems, typically millions during

the first out of two steps of the synthesis scheme. Saving data generated from these solutions causes the huge memory consumption. The data is then used in the second step, where aforementioned algorithms may be used to solve an auxiliary discrete problem. The latter steps classically execute sequentially, both in terms of theory and software implementation. To raise runtime performance methods for parallel execution (in theory [4], [8], [11] and in implementation [3]) have been presented recently. More concretely, the pioneering work [3] indicates the potential boost that can be achieved by utilizing high-performance computing platforms and [4], [8], [11] present theories for concurrent execution of the two steps.

Against this backdrop, the contribution of this paper is twofold. Firstly, we extend the class of solvable optimal control problems to problems, whose cost functions take negative values. Moreover, the presented algorithm allows for efficient implementation by parallelizing both the execution of the algorithm itself and the two steps of the synthesis scheme described above. In fact, we present a version of the well-known Bellman-Ford algorithm [12]–[14] for directed hypergraphs. The Bellman-Ford algorithm (on ordinary directed graphs) not only applies to negative edge weights; In contrast to the Dijkstra algorithm [15] it also allows parallelization relatively easily [16]. As we will show, the latter properties pass over to our novel variant. Moreover, we present a method to regulate the memory consumption during execution in the sense that processing speed can be traded for memory consumption. We particularly show that our algorithm outperforms in a concrete example the memory-efficient Dijkstra-like algorithm recently proposed in [4].

We will motivate the requirement of handling negative edge weights, which arise from arbitrary cost functions, by a practical example: automated aerial firefighting with an unmanned aerial vehicle. The firefighting aircraft shall not only reach the hot spot as fast as possible but shall be rewarded for flying over it as long as necessary in order to release its firefighting water. The existing theory on reach-avoid specifications is sufficient to reach the target while optimizing a non-negative cost function but insufficient to formulate a reward mechanism. We will set up a detailed scenario of aerial firefighting and thereby show the applicability of our theoretic results and the great performance of our algorithm.

The rest of the paper includes the notation used for presenting our theory in Section II. In Section III we summarize the existing theory about symbolic optimal control such that our main contributions, which are included in Section IV, can be presented rigorously. The application of our results to sampled-data systems are discussed in Section V and two

The authors are with the Munich University of Applied Sciences, Dept. of Mechanical, Automotive and Aeronautical Eng., 80335 München, Germany.

This work has been supported by the German Federal Ministry of Education and Research (Project ARCUS).

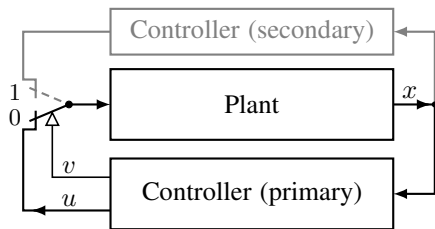


Fig. 1. Closed loop scheme [9] investigated in this work.

numerical examples are included in Section VI. A conclusion is given in Section VII.

II. NOTATION

The symbols \mathbb{R} , \mathbb{Z} and \mathbb{R}_+ , \mathbb{Z}_+ stand for the set of real numbers, integers and non-negative reals and integers, respectively. The symbol \emptyset denotes the empty set. For a map $f: A \rightarrow \mathbb{R}$ and $c \in \mathbb{R}$ the relations \leq , \geq hold point-wise, e.g. $f \geq c$ iff $f(a) \geq c$ for all $a \in A$. For f and another map $g: A \rightarrow \mathbb{R}$ we write $f \geq g$ iff $f(a) \geq g(a)$ for all $a \in A$. The derivative of a map f with respect to the first argument is denoted by D_1f . For sets A and B we denote the set of all functions $A \rightarrow B$ by B^A . A map with domain A and taking values in the powerset of B is denoted by $A \rightrightarrows B$. A set-valued map $f: A \rightrightarrows B$ is *strict* iff $f(a) \neq \emptyset$ for all $a \in A$. The cardinality of the set A is denoted by $|A|$.

III. THE NOTION OF SYSTEM AND OPTIMAL CONTROL

The class of optimal control problems that is considered in this work will be formalized in this section. To this end, we first introduce the notions of system, closed loop and controller. Then we define the notion of optimal control problem. We use herein the concepts introduced in [2], [10].

To summarize in advance, we investigate subsequently a closed loop scheme as depicted in Fig. 1: The primary controller is to be synthesized such that the total cost of the evolution of the closed loop is minimized. The total cost is obtained from accumulating running costs and adding a terminal cost instantaneously when the primary controller hands over the control to a secondary controller. The hand-over at some finite time is mandatory. (This scenario was rigorously defined in [9].)

A. System and Behavior

In this paper we use the following notion of system, which is frequently considered in literature in the following or similar variants, e.g. [2], [17], [18].

III.1 Definition. A *system* is a triple

$$(X, U, F), \quad (1)$$

where X and U are non-empty sets and $F: X \times U \rightrightarrows X$ is strict.

The first two components of a system S in (1) are called *state* and *input space*, respectively. The third component, the *transition function*, defines a dynamic evolution for the system through the difference inclusion

$$x(t+1) \in F(x(t), u(t)). \quad (2)$$

For example, a dynamical system obtained by discretizing an ordinary differential equation may be formulated as a system (1) with time-discrete dynamics (2). (See Section V-A for the details.) The *behavior* of S initialized at $p \in X$, which results from the imposed dynamics, is the set

$$\{(u, x) \in (U \times X)^{\mathbb{Z}_+} \mid p = x(0) \wedge \forall t \in \mathbb{Z}_+: (2) \text{ holds}\}. \quad (3)$$

Loosely speaking, the behavior is the set of all input-output signal pairs that can be measured on the lines of the system. Subsequently, we denote (3) by $\mathcal{B}_p(S)$.

B. Controller and Cost functional

We investigate the problem of synthesizing an optimal controller with respect to costs as we detail below. To begin with, by a *controller* for a system S of the form (1) we mean a strict set-valued map

$$\mu: X \rightrightarrows U.$$

Therefore, controllers in this work are static, do not block, and do not use information from the past. By concept, a controller shall restrict the behavior of the plant to control. This property is reflected in our formalism as follows. We define the *closed-loop behavior* of the controller μ interconnected with S and initialized at $p \in X$ by

$$\mathcal{B}_p^\mu(S) = \{(u, x) \in \mathcal{B}_p(S) \mid \forall t \in \mathbb{Z}_+ u(t) \in \mu(x(t))\}. \quad (4)$$

Obviously, $\mathcal{B}_p^\mu(S) \subseteq \mathcal{B}_p(S)$, so this formalism is indeed compliant with intuition about controllers.

The objective that we consider is to minimize the cost for operating the closed loop. Specifically, given a *terminal* and *running cost function* of the form

$$G: X \rightarrow \mathbb{R} \cup \{\infty\}, \quad \text{and} \quad (5a)$$

$$g: X \times X \times U \rightarrow \mathbb{R} \cup \{\infty\}, \quad (5b)$$

respectively, the controller shall minimize the cost functional

$$J: (U \times \{0, 1\} \times X)^{\mathbb{Z}_+} \rightarrow \mathbb{R} \cup \{-\infty, \infty\}$$

defined as follows:

$$J(u, v, x) = G(x(T)) + \sum_{t=0}^{T-1} g(x(t), x(t+1), u(t)) \quad (6)$$

if $T := \inf v^{-1}(1) < \infty$ and $J(u, v, x) = \infty$ if $v = 0$. In words, v is a boolean-valued signal whose first edge from 0 to 1 defines the termination time T of the (primary) controller. We would like to illustrate the notion of cost by the following example. It will be also continued later.

III.2 Example. Let (X, U, F) be a system with seven states and two inputs, where F is defined graphically in Fig. 2. To be specific, $X = \{1, 2, \dots, 7\}$, $U = \{b, g\}$ and the black and gray dashed edges, respectively, define the image of F for the input b and g , respectively. E.g., $F(1, b) = \{1\}$, $F(4, g) = \{1, 2\}$. The running cost function g is also defined graphically by the label of each edge. E.g., $g(1, 1, b) = 1$, $g(2, 3, g) = -4$. The terminal cost function G is defined by $G(x) = x$ for all $x \in X$, i.e. the label of a state in Fig. 2

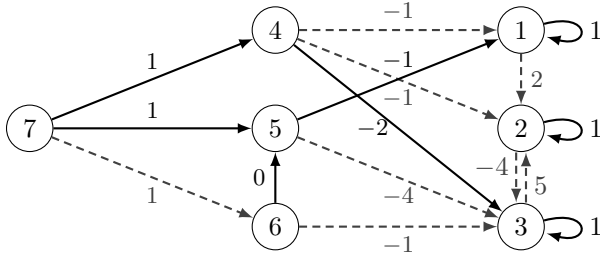


Fig. 2. System and cost functions in Examples III.2, III.3 and IV.1.

equals exactly the value of the terminal cost of the state. We consider the state and input signal $x = (7, 4, 3, 3, \dots)$ and $u = (b, b, \dots)$, and the termination signals $v_0 := (1, \dots)$, $v_1 := (0, 1, \dots)$ and $v_2 := (0, 0, 1, \dots)$. Then, $J(u, v_0, x) = G(7) = 7$, $J(u, v_1, x) = G(4) + g(7, 4, b) = 4 + 1$ and $J(u, v_2, x) = 3 + 1 - 2 = 2$. Analogously, for $y = (7, 5, 1, 1, \dots)$ it holds $J(u, v_1, y) = 6$, $J(u, v_2, y) = 1$. \square

To a controller μ we associate a *closed-loop performance initialized at* $p \in X$, which is the value

$$L(p, \mu) = \sup_{(u, x) \in \mathcal{B}_p^\mu(S)} \inf \{J(u, v, x) \mid v \in \{0, 1\}^{\mathbb{Z}^+}\}. \quad (7)$$

Roughly speaking, this quantity is the *worst-case* cost for the evolution of the closed loop with controller μ for the *best* possible hand-over time $T = \inf v^{-1}(1)$. We would like to illustrate the closed-loop performance of a controller by continuing Example III.2.

III.3 Example. Let the system $S := (X, U, F)$, the cost functions G, g and u, v_2, x, y be as in Example III.2. We consider the controller $\mu: X \rightrightarrows U$ defined by $\mu(x) = \{b\}$ for all $x \in X$. Then $\mathcal{B}_7^\mu(S) = \{(u, x), (u, y)\}$. Hence, using the results in Example III.2 we conclude that the closed-loop performance initialized at 7 satisfies $L(7, \mu) = \max\{J(u, v_2, x), J(u, v_2, y)\} = \max\{1, 2\} = 2$. Note that a termination time greater than 2 increases the cost by 1 since $g(1, 1, b) = g(3, 3, b) = 1$. \square

C. Optimal Control Problem

The previously defined objects in (1) and (5) can be grouped together in a compact form [9].

III.4 Definition. Let S be a system of the form (1). An *optimal control problem* (on S) is a 5-tuple

$$(X, U, F, G, g) \quad (8)$$

where G and g are as in (5).

Finally, we relate the solution of an optimal control problem Π of the form (8) to the so-called *value function*. The latter is the map $V: X \rightarrow \mathbb{R} \cup \{-\infty, \infty\}$ defined by

$$V(p) = \inf \{L(p, \nu) \mid \nu: X \rightrightarrows U \text{ strict}\}. \quad (9)$$

We say that $\mu: X \rightrightarrows U$ realizes V if $V = L(\cdot, \mu)$. If additionally $V(p)$ is finite for all $p \in A$, where $A \subseteq X$, then μ is *optimal* for Π on A . (Here, optimal controller and optimal termination are formally separated, see (7). However, as we will see later, both come naturally hand in hand.)

The focus of this work is on how to solve optimal control problems of the form (8) algorithmically. Therefore, we shall review some important results on optimal control problems. In fact, we will use [19, Th. IV.2] in the proofs of our main results later. It states that the value function is the maximal fixed point of the *dynamic programming operator* $P: [-\infty, \infty]^X \rightarrow [-\infty, \infty]^X$ defined by

$$P(W)(x) = \min \left\{ G(x), \inf_{u \in U} \sup_{y \in F(x, u)} g(x, y, u) + W(y) \right\}. \quad (10)$$

The precise statement is as follows.

III.1 Theorem. Let Π be an optimal control problem of the form (8) and let V be the value function of Π defined in (9). Then V is the maximal fixed point of the functional defined in (10), i.e. $P(V) = V$ and if $W \leq P(W)$ then $W \leq V$ for every $W \in [-\infty, \infty]^X$.

We would like to emphasize that the previous setup can be easily rephrased to the terminology of directed hypergraphs and the search for optimal (hyper-)paths. In fact, we may identify a system (with the input space being a singleton) with a directed hypergraph, where every hyperarc points to possibly several vertices [20]. This is the very reason that graph-theoretical algorithms can be used as a computational means to obtain controllers. Subsequently, we present such an algorithm.

IV. MAIN CONTRIBUTIONS

In this section, we present our main contribution, which is an algorithm to determine the value function and the realizing controller under weaker assumptions than so far known on the given optimal control problem. Specifically, for the special case that terminal and running cost functions satisfy $G, g \geq 0$ a generalized Dijkstra algorithm was presented in [10] to solve the optimal control problem. (Various versions of the Dijkstra algorithm were used also in other works like [11], [21]–[23].) Besides the restriction to non-negative cost functions the Dijkstra algorithm has another disadvantage according to the prevailing opinion in literature: it cannot be conveniently parallelized due to the involved priority queue.

The novel algorithm we present below does not require the non-negativity of G nor of g , and it can be easily executed in parallel. In the special case of ordinary, directed graphs the novel algorithm reduces to the classical Bellman-Ford algorithm [12] combined with ideas of Yen [24] and Cormen et. al. [25]. Using the techniques of the latter works a memory and time efficient implementation can be realized. The classical Bellman-Ford algorithm can be executed with a high degree of parallelism [16], [26], and our algorithm inherits this property. We discuss implementation details in Section IV-B. In Section IV-A, we present the algorithm and its properties.

A. Algorithm

In the statement of Algorithm 1 the set

$$\text{pred}(x, u) = \{y \in X \mid x \in F(y, u)\} \quad (11)$$

is used, which may be seen as the preimages of F or, equivalently, as the predecessors in the hypergraph defined by F . (In (11), F and X are as in Algorithm 1.) Algorithm 1

Algorithm 1 Generalized Bellman-Ford-Yen Algorithm

Input: Optimal control problem (X, U, F, G, g)

```

1:  $\mathcal{F}_1 \leftarrow \emptyset$  // "Active" Frontier [25]
2:  $\mathcal{F}_2 \leftarrow \emptyset$  // "Upcoming" Frontier [25]
3: for all  $x \in X$  do
4:    $W(x) \leftarrow G(x)$ 
5:    $\mu(x) \leftarrow U$ 
6:   if  $G(x) < \infty$  then
7:      $\mathcal{F}_1 \leftarrow \mathcal{F}_1 \cup (\cup_{u \in U} \text{pred}(x, u))$ 
8:   end if
9: end for
10:  $i = 0$ 
11: while  $\mathcal{F}_1 \neq \emptyset$  and  $i < |X|$  do
12:   for  $(x, u) \in \mathcal{F}_1 \times U$  do
13:      $d \leftarrow \sup_{y \in F(x, u)} g(x, y, u) + W(y)$ 
14:     if  $d < W(x)$  then
15:        $W(x) \leftarrow d$ 
16:        $\mu(x) \leftarrow \{u\}$ 
17:        $\mathcal{F}_2 \leftarrow \mathcal{F}_2 \cup (\cup_{\tilde{u} \in U} \text{pred}(x, \tilde{u}))$ 
18:     end if
19:   end for
20:    $\mathcal{F}_1 \leftarrow \mathcal{F}_2$  // Swap frontiers
21:    $\mathcal{F}_2 \leftarrow \emptyset$ 
22:    $i \leftarrow i + 1$ 
23: end while
24: return  $W, \mu$ 

```

basically implements a fixed-point iteration according to (10) using additionally some heuristics to improve efficiency, which we adopt from improvements on the classical Bellman-Ford algorithm [27]. Firstly, Yen [24] observed that only a certain subset of predecessors need to be processed iteratively in the while-loop – and not all elements of X . Secondly, in [25] the two sets \mathcal{F}_1 and \mathcal{F}_2 , which are called *frontiers*, have been introduced replacing the queue proposed in [24]. Lastly, the second condition in line 11 implements negative cycle detection.

IV.1 Theorem. *Let S be a system of the form (1), where X and U are finite. Let Π be an optimal control problem of the form (8) on S . If Algorithm 1 terminates with $\mathcal{F}_1 = \emptyset$ then W equals the value function of Π and μ realizes W .*

Before we give the proof of the theorem and discuss the time complexity of the algorithm, we would like to briefly illustrate its execution in a simple example.

IV.1 Example. Let (X, U, F, G, g) be the optimal control problem defined by means of Example III.2. We apply Algorithm 1 to it. After initialization (line 9) the frontier \mathcal{F}_1 equals X as every state is a predecessor of some state. Starting the for-loop in line 12 with $(x, u) = (6, b)$ lines 15, 16 imply $W(6) = 0 + W(5) = 5$ and $\mu(6) = \{b\}$. (Note that the processing order for \mathcal{F}_1 is irrelevant.) Then

$\mathcal{F}_2 = \text{pred}(6, g) = \{7\}$ in line 17. The next iteration with $(x, u) = (6, g)$ results in the changes $W(6) = -1 + W(3) = 2$ and $\mu(6) = \{g\}$. Executing the for-loop in line 12 again for $(x, u) = (4, g)$ yields $W(4) = -1 + \max\{W(1), W(2)\} = -1 + \max\{1, 2\} = 1$ as $F(4, g) = \{1, 2\}$. Analogously, we update $W(5) = W(2) = -1$ and when exiting the for-loop (line 19) all but the state 5 need to be processed again. In fact, $\mathcal{F}_2 = X \setminus \{5\}$ as the W -values of $\{1\} = F(5, b)$ and $\{3\} = F(5, g)$ do not change. The following execution of the while-loop (line 11) is therefore done with $\mathcal{F}_1 = X \setminus \{5\}$. Continuing the execution as illustrated until $\mathcal{F}_1 = \emptyset$ we finally obtain that the optimal controller μ satisfies $\mu(6) = \{b\}$ and $\mu(s) = \{g\}$ for $s \in \{2, 4, 5, 7\}$. For states 1 and 3 the image of μ is U , which may be interpreted as the command to hand over control. \square

Proof of Theorem IV.1. Denote by V the value function of Π and let P be as in (10). We shall prove $W = V$. Assume that the inequality $\tilde{V}(x) > P(\tilde{V})(x)$ holds for some $x \in X$, where \tilde{V} denotes the intermediate value of W at the end of the for-loop in line 19 at some iteration. Then there exists $u \in U$ such that $W(y) < \infty$ for all $y \in F(x, u)$. So $x \in \mathcal{F}_2$, which implies $\tilde{V}(x) = P(\tilde{V})(x)$ in the next iteration. This proves $W \leq P(W)$ and therefore $W \leq V$ by Theorem III.1. Since $W \geq P(W) \geq P(V) = V$ by lines 4, 15 and Theorem III.1 we conclude $W \geq V$ and therefore $W = V$. The claim on μ is obvious. \square

IV.2 Theorem. *Algorithm 1 can be implemented to run with time complexity $\mathcal{O}(nm)$, where $n = |X|$ and $m = \sum_{(x, u) \in X \times U} |F(x, u)|$.*

Proof. The while-loop in Algorithm 1 is executed at most n times and the nested for-loop at most m times, which proves the claim. \square

B. Implementation technique

Section IV is concluded with some notes on how to implement Algorithm 1 efficiently.

The frontiers \mathcal{F}_1 and \mathcal{F}_2 can be realized as FIFO queues such that their lengths never exceed $|X|$. As for parallelization, it is readily seen that the for-loop in lines 12-19 can be executed in parallel where only the reading (resp. writing) operation on the array W in line 13 (resp. line 15) needs to be thread-safe. In this case, every thread uses its own local frontier \mathcal{F}_2 to avoid further communication among the threads. All local frontiers are finally merged to obtain \mathcal{F}_1 .

Memory consumption can be controlled quite easily. Firstly, only \mathcal{F}_1 , \mathcal{F}_2 , W and μ need to reside in memory throughout execution. Keeping the images of F and pred in memory throughout execution normally results in increased processing speed. Reading the data out of memory is typically faster than computing the images. On the other hand, these data significantly contribute to the memory consumption. Therefore, in case of the lack of memory, recomputing images of F and pred allows to continue the execution. Needless to say, the computation method for F and pred depends on the representation of the input data.

V. APPLICATION TO SAMPLED SYSTEMS

Within the framework of symbolic optimal control Algorithm 1 can be used for synthesizing near-optimal controllers for sampled-data systems with continuous state space. Specifically, the sampled version of a dynamical system with continuous-time continuous-state dynamics

$$\dot{x}(t) = f(x(t), u(t)) \quad (12)$$

can be considered. In (12), f is a function $\mathbb{R}^n \times \bar{U} \rightarrow \mathbb{R}^n$, where $\bar{U} \subseteq \mathbb{R}^m$, $n, m \in \mathbb{N}$.

A brief overview of the synthesis method is given below in preparation for our experimental results in Section VI. More concretely, in Section V-A *sampled systems* are formalized and then *discrete abstractions* are introduced. The technique to implement a synthesis algorithm for control problems on sampled systems is outlined in Section V-B.

A comprehensive discussion of symbolic control is beyond the scope of this paper. The interested reader may refer to [2] for further details.

A. Symbolic near-optimal control of sampled systems

In this work, we assume in (12) that $f(\cdot, \bar{u})$ is locally Lipschitz-continuous for all $\bar{u} \in \bar{U}$ and $\text{dom } \varphi = \mathbb{R}_+ \times \mathbb{R}^n \times \bar{U}$. Here and subsequently, the symbol φ is used to denote the general solution of (12), i.e. $\varphi(0, x, u) = x$ and $D_1\varphi(t, x, u) = f(\varphi(t, x, u), u)$ for all $(t, x, u) \in \text{dom } \varphi$.

We may formulate the discretization of (12) with respect to a chosen sampling time τ as below [2].

V.1 Definition. Let $\tau > 0$. A system S of the form (1) with $X = \mathbb{R}^n$, $U = \bar{U}$ is called **sampled system** associated with f and τ if $F(x, u) = \{\varphi(\tau, x, u)\}$ for all $(x, u) \in X \times U$.

Given an optimal control problem Π of the form (8), where $S = (X, U, F)$ is a sampled system, the theory developed in [10] implies a method to be outlined below to compute near-optimal controllers. Here, we say a controller μ for Π is *near-optimal on* $A \subseteq X$, if its closed-loop performance (7) is finite on A , i.e. $L(p, \mu) < \infty$ for all $p \in A$. The term “near-optimal” can be indeed justified since according to the theory of symbolic optimal control [10] the considered synthesis method implies a sequence of functions converging to the value function of the problem. It is beyond the scope of this paper to investigate the convergence properties in detail.

In the first step of the aforementioned method a certain auxiliary optimal control problem $\Pi' = (X', U', F', G', g')$ is defined. By virtue of its special properties, which we explain later, theory ensures that a near-optimal controller for the actual control problem is found if Π' can be solved. The latter statement is the key point of this synthesis method: Π' is chosen having *discrete* problem data and is solved in the second step. So, algorithms, as the one we have presented, can be used to eventually obtain a controller for the actual control problem. The structure of the controller for the actual problem is explained after the discussion of Π' .

The key object in Π' is the so-called discrete abstraction. A discrete abstraction is, roughly speaking, an approximation of the system dynamics: The continuous state space of the

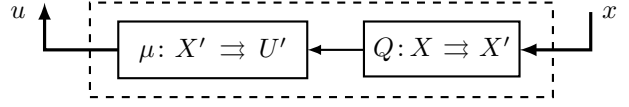


Fig. 3. Structure of the controller $X \Rightarrow U$ for optimal control problem Π in Section V-A. The controller is the composition of μ and Q , where μ is an optimal controller for the auxiliary problem Π' and the quantizer Q is given through the property $\Omega \in Q(x) \Leftrightarrow x \in \Omega$.

given sampled system is quantized by means of a cover, a subset of the input space is picked and transitions between the elements of the cover for the few chosen inputs “cover” the transition function of the sampled system. The precise definition of a discrete abstraction is the following [2].

V.2 Definition. Let S be a sampled system and let the system $S' = (X', U', F')$ satisfy:

- 1) X' is a cover of X by non-empty sets;
- 2) $U' \subseteq U$;
- 3) Let $\Omega_i \in X$, $i \in \{1, 2\}$, $u \in U'$. If $\Omega_2 \cap F(\Omega_1, u) \neq \emptyset$ then $\Omega_2 \in F'(\Omega_1, u)$.

Then S' is called a **discrete abstraction** of S .

The correctness of previous method is based on the following “overapproximation” properties of Π' :

- 1) $G(x) \leq G'(\Omega)$, whenever $x \in \Omega \in X'$;
- 2) $g(x, x', u) \leq g'(\Omega, \Omega', u)$, whenever $u \in U'$, $(x, x') \in (\Omega, \Omega') \in X' \times X'$;
- 3) The system (X', U', F') is a discrete abstraction of S .

The structure of the controller μ for S is simple: It is composed of the optimal controller for Π' and the quantizer induced by the cover X' . See Fig. 3.

B. Implementation of Symbolic Optimal Control

In order to solve optimal control problems in practice sophisticated choices for the ingredients of the discrete abstraction are required. In this paper, we implement the method of [2], [28] in the following sense. Let S be the sampled system associated with f and τ . A discrete abstraction (X', U', F') of S is constructed as follows. The set X' consists of a finite number of compact hyper-rectangles and a finite number of unbounded sets such that X' is a cover of X . The compact sets in X' are translated copies of

$$[0, \eta_1] \times \cdots \times [0, \eta_n]$$

for some parameter $\eta \in \mathbb{R}_+^n$. Typically, these compact elements cover the “operating range” of the controller to synthesize whereas the other elements catch “overflows”. Some finite subset $U' \subseteq U$ is chosen. Condition 3) in Definition V.2 is realized by overapproximating the attainable sets $\varphi(\tau, \Omega, \bar{u})$ for $(\Omega, \bar{u}) \in X' \times U'$ by hyper-rectangles [29]. Applying Algorithm 1 to discrete abstractions is straightforward by observing that the algorithm remains correct if pred is replaced by a superset of it. Such a set can be obtained for a sampled system by integrating the time-reverse dynamics

$$\dot{x}(t) = -f(x(t), u(t)) \quad (13)$$

and overapproximating attainable sets accordingly [4].

VI. EXAMPLES

We discuss a detailed problem about aerial firefighting in Section VI-A and compare the performance of our algorithm to the Dijkstra-like algorithm of [4] in Section VI-B.

A. Automated aerial firefighting

Until now, only few scientific works discuss automated aerial firefighting. The works [30], [31] focus on quadcopters and their properties for firefighting. The work [32] discusses a leader-follower firefighting strategy based on engineering experience. At the same time, automated aerial firefighting would drastically increase efficiency of the firefighting task while reducing risk for humans. The reasons are divers: One main difficulty in extinguishing wildfires is that aerial firefighting in darkness is typically not possible for the sake of pilots' safety. So a considerable amount of time is lost. In any case, firefighting pilots take a huge risk in those operations due to turbulence, smoke, other participating vehicles and the like. Therefore, firefighting unmanned aerial vehicles in combination with a sophisticated firefighting strategy would reduce risks for humans.

As one next step towards automated aerial firefighting we apply in this section our novel results of Section IV to a simplified scenario of a wildfire: An aircraft fights the fire by releasing its water tank over the hot spot. It is not our purpose to present a fully realistic scenario that includes real problem data. Nevertheless the presented scenario is scalable to real data and the full potential of symbolic controller synthesis is also not exploited for the sake of a clear presentation. For example, uncertainties due to wind or sensor noise could be easily taken into account [2, Sect. VI-B] but would add some extra notation.

1) *Problem definition:* We consider a fixed-wing aircraft, where we model a) the planar motion of the aircraft, b) instantaneous weight loss due to water release. In fact, we consider equations of motion given by (12) with f_1 ("empty water tank"), respectively f_2 ("filled water tank"), in place of f . Here, $f_\sigma: \mathbb{R}^4 \times \bar{U} \rightarrow \mathbb{R}^4$ with $\sigma \in \{1, 2\}$ is given by

$$f_\sigma(x, u) = \begin{pmatrix} x_4 \cdot \cos(x_3) \\ x_4 \cdot \sin(x_3) \\ m_\sigma^{-1} \cdot p_L \cdot x_4 \cdot \sin(u_2) \\ m_\sigma^{-1}(u_1 - p_D \cdot x_4^2) \end{pmatrix}, \quad (14)$$

where \bar{U} and the symbols in (14) are explained in Tab. I. This point-mass model for a fixed-wing aircraft is widely used in literature, e.g. [33, Sect. 3].

The specification is to fly the aircraft to the fire after departure from the airfield, fly over the fire for some "optimal" time and fly back to the airfield. Obstacles in the area must be avoided and the aircraft must be flown within allowed limits. The relevant sets of the scenario are given in Tab. II. See also Fig. 4.

We formalize this mission by two optimal control problems $\Pi_i = (X, U, F_i, G_i, g_i)$, $i \in \{1, 2\}$ which we are going to solve in succession. The optimal control problem Π_1 is the control task to fly from the fire back to the airfield with

Symbol	Meaning and numerical values where applicable
(x_1, x_2)	Planar position of aircraft
x_3	Heading of aircraft
x_4	Velocity of aircraft
u_1	Thrust of aircraft
u_2	Bank angle of aircraft
\bar{U}	Admissible range of thrust and bank angle; $\bar{U} = [0, 18 \cdot 10^3] \times [-40^\circ, 40^\circ]$
m_1 m_2	Mass of aircraft without [with] its payload; $m_1 = 4250$, $m_2 = 6250$
p_D	Coefficient (rel. to drag) in aircraft dynamics; $p_D = 1.8$
p_L	Coefficient (rel. to lift) in aircraft dynamics; $p_L = 85$

TABLE I
SYMBOLS USED IN (14).

Symbol	Value	Meaning
X_{scen}	$[0, 2500] \times [0, 800]$	Spatial mission area
\bar{X}	$X_{\text{scen}} \times \mathbb{R} \times [50, 85]$	Operating range of controllers
A_{rwy}	$[300, 900] \times [100, 180]$	Runway of the airfield
A_{land}	$[-10^\circ, 10^\circ] \times [50, 55]$	Admissible heading and velocity of aircraft for landing
A_{fire}	$\subseteq \mathbb{R}^2$, see Fig. 4	Water release region (fire)
A_{drop}	$\mathbb{R} \times [53, 56]$	Admissible heading and velocity of aircraft for water release
A_{nofly}	$[320, 880] \times [120, 160] \times [12^\circ, 348^\circ] \times \mathbb{R}$	Illegal aircraft states over runway
A_{hill}	$\subseteq \mathbb{R}^2$, see Fig. 4	Spatial obstacle set
A_a	$A_{\text{nofly}} \cup (A_{\text{hill}} \times \mathbb{R}^2)$	Overall obstacle set

TABLE II
SETS DEFINING THE SCENARIO.

empty water tank. In particular, (X, U, F_1) is the sampled system associated with f_1 and sampling time $\tau = 0.45$, and

$$g_1(x, y, u) = \begin{cases} \infty, & \text{if } y \in (\mathbb{R}^4 \setminus \bar{X}) \cup A_a \\ \tau + u_2^2, & \text{otherwise} \end{cases}$$

$$G_1(x) = \begin{cases} \infty, & \text{if } x \notin A_{\text{rwy}} \times A_{\text{land}} \\ 0, & \text{otherwise} \end{cases}$$

Loosely speaking, the optimal controller for Π_1 minimizes the time to arrive at the airfield but additionally favors small bank angles¹ and avoids obstacles. The controller terminates its action only if the aircraft is on "final approach", which is enforced by G_1 .

Optimal control problem Π_2 formalizes the control task to fly to the hot spot with filled water tank. In particular, (X, U, F_2) is the sampled system associated with f_2 and τ ,

$$g_2(x, y, u) = \begin{cases} -5\tau, & \text{if } y \in A_{\text{fire}} \times A_{\text{drop}} \\ g_1(x, y, u), & \text{otherwise} \end{cases}$$

and $G_2 = V_1$, where V_1 is the value function of Π_1 . The motivation for g_2 is to reward the aircraft for flying over the fire. The controller terminates its action at a beneficial state for flying back to the airfield. The latter behavior is due to the definition of G_2 .

2) *Auxiliary optimal control problems:* To solve Π_1 and Π_2 two auxiliary problems $\Pi'_i = (X', U', F'_i, G'_i, g'_i)$, $i \in \{1, 2\}$ are defined in accordance with Section V, where the ingredients are as follows. The "abstract" state and input space satisfy $|X'| \approx 141.7 \cdot 10^6$ and $|U'| = 35$, respectively.

¹In the definition of g_1 , angles are taken in radians in the range $[-\pi, \pi]$.

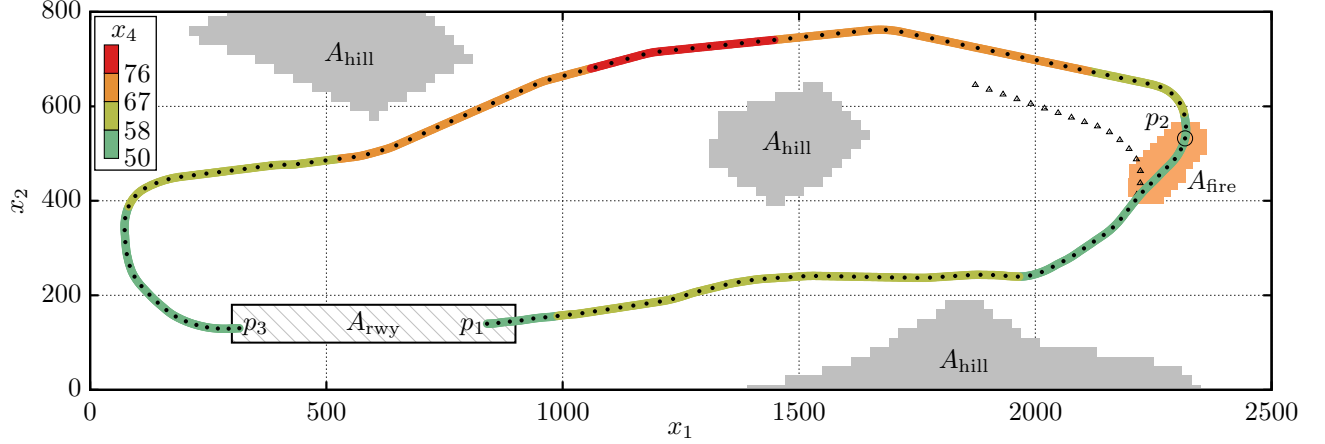


Fig. 4. Aerial firefighting scenario from Section VI-A. A closed-loop trajectory is illustrated, which starts at $p_1 = (840, 140, 0^\circ, 53)$ and ends at $p_2 \approx (319, 130, 2.43^\circ, 50.4)$. At the point p_2 (\odot) the controller for Π_2 hands over the control to the controller for Π_1 . The trajectory segment indicated by the triangles belongs to a trajectory that would result if for both Π_1 and Π_2 the running cost be equal to g_1 , i.e. without reward mechanism.

They are defined through subdividing the components of $X_{\text{scen}} \times [-\pi, \pi] \times [50, 85]$ and \bar{U} into $200 \cdot 70 \cdot 75 \cdot 135$ and $4 \cdot 6$ respectively, compact hyper-rectangles. The running costs are defined by

$$g'_1(\Omega, \Omega', u) = \begin{cases} \infty, & \text{if } \Omega' \cap ((\mathbb{R}^4 \setminus \bar{X}) \cup A_a) \neq \emptyset \\ \tau + u_2^2, & \text{otherwise} \end{cases}$$

$$g'_2(\Omega, \Omega', u) = \begin{cases} -5\tau, & \text{if } \Omega' \subseteq A_{\text{fire}} \times A_{\text{drop}} \\ g'_1(\Omega, \Omega', u), & \text{otherwise} \end{cases}$$

and the terminal costs by $G'_2 = V'_1$,

$$G'_1(\Omega) = \begin{cases} 0, & \text{if } \Omega \subseteq A_{\text{rwy}} \times A_{\text{land}} \\ \infty, & \text{otherwise} \end{cases}$$

where V'_1 is the value function of Π'_1 .

3) *Experimental results:* Both Π'_1 and Π'_2 can be solved utilizing Algorithm 1 and near-optimal controllers for Π_1 on $A_{\text{fire}} \times A_{\text{drop}}$ and for Π_2 on $A_{\text{rwy}} \times A_{\text{land}}$ are found. A trajectory of the resulting closed loop is illustrated in Fig. 4. It is also important to note that the reward mechanism implemented by means of g_2 is indeed relevant to fly the aircraft a longer time over the fire. Disabling this mechanism, i.e. defining Π_2 with g_1 in place of g_2 , results in the trajectory outlined by the triangles in Fig. 4. Hence, the hand-over command would follow immediately after reaching A_{fire} .

The performance of Algorithm 1 shall be discussed by means of Fig. 5. The corresponding implementation is written in C and compiled for Linux.

Firstly, Fig. 5a indicates that the load of the random access memory can be regulated almost without restrictions. Specifically, the used implementation stores all computed images of F and pred until 68% of RAM is consumed (predefined by user). After that, after every iteration (line 19 in Algorithm 1) all transitions are deleted from memory except those required in the next iteration. A temporary small loss of processing speed can be detected but the computation proceeds efficiently.

Fig. 5b illustrates the great scaling property of the algorithm (and its implementation) with respect to parallelization.

B. Aircraft landing maneuver

We would like to compare the performance of Algorithm 1 with the one of a recent, memory-efficient Dijkstra-like algorithm. To be specific, we apply our algorithm to the example considered in [4, Sect. V.B], which is a control problem about landing an aircraft DC-9 with 3-dimensional dynamics. Algorithm 1 of this paper needs 122 MB memory, which is 61% less than the consumption reported for “Algorithm 2” of [4] (317 MB). With one thread (resp. two threads) the computation terminates successfully in 321 (resp. 255) seconds². The authors of [4] report 320 seconds runtime, where only sequential computation is feasible.

VII. CONCLUSIONS

Our experimental results confirm the conclusions in [3] that the efficiency of symbolic controller synthesis can be drastically increased by utilizing algorithms that can be executed in parallel. In addition, our second numerical example reveals that though Dijkstra-like algorithms have a smaller time complexity than our algorithm the ability of parallelization and limiting RAM usage makes our algorithm more suitable for solving complex control problems. The aerial firefighting problem in Section VI-A could not be solved, or could not be solved in a reasonable time, without the said properties.

In future work further techniques for an even higher degree of parallelization will be investigated, e.g. using graphical processing units. On such an architecture thousands of elementary operations can be executed in parallel. The challenge is to organize shared memory operations properly since they take a significant amount of runtime.

²Implementation and hardware as in Section VI-A.

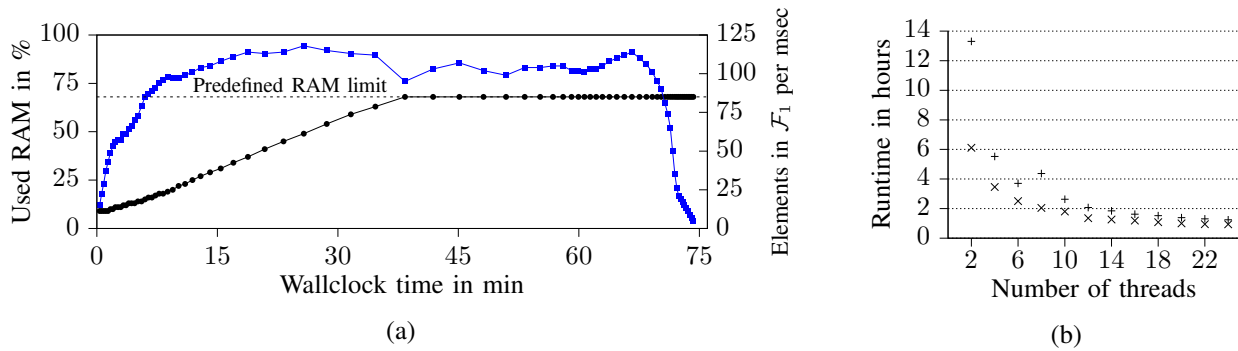


Fig. 5. Performance analysis of Algorithm 1 and its implementation applied to the optimal control problems in Section VI-A. All computations ran on up to 24 CPUs of type Intel Xeon E5-2697 v3 (2.60GHz) sharing 64 GB RAM. (a) Relation between memory use (●) and processing speed (■) when solving Π'_2 using 24 threads. The quantities are measured whenever the for-loop in Algorithm 1 is exited (line 19). For RAM usage the system function `getrusage` [34] is used. (b) Runtime in dependence of the number of threads that are used to solve problem Π'_1 (×) and Π'_2 (+), respectively.

ACKNOWLEDGMENT

The authors gratefully acknowledge the compute resources provided by the Leibniz Supercomputing Centre.

REFERENCES

- [1] P. Tabuada, *Verification and control of hybrid systems*. New York: Springer, 2009.
- [2] G. Reissig, A. Weber, and M. Rungger, “Feedback refinement relations for the synthesis of symbolic controllers,” *IEEE Trans. Automat. Control*, vol. 62, no. 4, pp. 1781–1796, Apr. 2017.
- [3] M. Khaled and M. Zamani, “pFaces*: An acceleration ecosystem for symbolic control,” in *Proc. 22th Intl. Conf. Hybrid Systems: Computation and Control (HSCC), Montreal, Canada, Apr. 16-18, 2019*. Springer.
- [4] E. Macoveiciuc and G. Reissig, “Memory efficient symbolic solution of quantitative reach-avoid problems,” in *Proc. American Control Conference (ACC)*, July 2019, pp. 1671–1677.
- [5] O. Maler, A. Pnueli, and J. Sifakis, “On the synthesis of discrete controllers for timed systems,” in *Annual Symposium on Theoretical Aspects of Computer Science*. Springer, 1995, pp. 229–242.
- [6] R. Bloem, B. Jobstmann, N. Piterman, A. Pnueli, and Y. Sa’ar, “Synthesis of reactive(1) designs,” *J. Comput. System Sci.*, vol. 78, no. 3, pp. 911–938, 2012.
- [7] A. Girard, “Controller synthesis for safety and reachability via approximate bisimulation,” *Automatica J. IFAC*, vol. 48, no. 5, pp. 947–953, 2012.
- [8] K. Hsu, R. Majumdar, K. Mallik, and A. Schmuck, “Lazy abstraction-based control for safety specifications,” in *2018 IEEE Conf. on Decision and Control (CDC)*, Dec. 2018, pp. 4902–4907.
- [9] G. Reissig and M. Rungger, “Abstraction-based solution of optimal stopping problems under uncertainty,” in *Proc. IEEE Conf. Decision and Control (CDC), Florence, Italy, 10-13 Dec. 2013*. New York: IEEE, 2013, pp. 3190–3196.
- [10] —, “Symbolic optimal control,” *IEEE Trans. Automat. Control*, 2018.
- [11] M. Rungger and O. Stursberg, “On-the-fly model abstraction for controller synthesis,” in *Proc. American Control Conference (ACC)*, 2012, pp. 2645–2650.
- [12] R. Bellman, “On a routing problem,” *Quart. Appl. Math.*, vol. 16, no. 1, pp. 87–90, 1958.
- [13] L. R. Ford, “Network flow theory,” RAND Corp Santa Monica, CA, USA, Tech. Rep., 1956.
- [14] E. F. Moore, “The shortest path through a maze,” in *Proc. Int. Symp. on the Theory of Switching*. Harvard Univ. Press, 1959, pp. 285–292.
- [15] E. W. Dijkstra, “A note on two problems in connexion with graphs,” *Numerische Mathematik*, vol. 1, no. 1, pp. 269–271, 1959.
- [16] F. Busato and N. Bombieri, “An efficient implementation of the bellman-ford algorithm for kepler GPU architectures,” *IEEE Trans. on Parallel and Distributed Systems*, vol. 27, no. 8, pp. 2222–2233, 2016.
- [17] A. Girard, “Synthesis using approximately bisimilar abstractions: state-feedback controllers for safety specifications,” in *Proc. 13th Intl. Conf. Hybrid Systems: Computation and Control (HSCC)*, 2010, pp. 111–120.
- [18] M. Rungger and M. Zamani, “SCOTS: a tool for the synthesis of symbolic controllers,” in *Proc. 19th Intl. Conf. Hybrid Systems: Computation and Control (HSCC)*. ACM, 2016, pp. 99–104.
- [19] G. Reissig, “Approximate value iteration for a class of deterministic optimal control problems with infinite state and input alphabets,” in *2016 IEEE 55th Conf. on Decision and Control (CDC)*. IEEE, Dec. 2016, pp. 1063–1068.
- [20] G. Ausiello, A. D’Atri, and D. Sacca, “Minimal representation of directed hypergraphs,” *SIAM Journal on Computing*, vol. 15, no. 2, pp. 418–431, 1986.
- [21] L. Grüne and O. Junge, “Global optimal control of perturbed systems,” *J. Optim. Theory Appl.*, vol. 136, no. 3, pp. 411–429, 2008.
- [22] G. Reißig, “Computing abstractions of nonlinear systems,” *IEEE Trans. Automat. Control*, vol. 56, no. 11, pp. 2583–2598, Nov. 2011.
- [23] A. Weber and G. Reissig, “Strongly convex attainable sets and low complexity finite-state controllers,” in *Proc. Australian Control Conf. (AUCC), Perth, Australia, 4-5 Nov. 2013*, 2013, pp. 61–66.
- [24] J. Y. Yen, “An algorithm for finding shortest routes from all source nodes to a given destination in general networks,” *Quart. Appl. Math.*, vol. 27, no. 4, pp. 526–530, 1970.
- [25] T. H. Cormen, C. E. Leiserson, R. L. Rivest, and C. Stein, *Introduction to algorithms*. Cambridge, MA, USA: MIT Press, Cambridge, MA, 2009.
- [26] A. Davidson, S. Baxter, M. Garland, and J. D. Owens, “Work-efficient parallel GPU methods for single-source shortest paths,” in *2014 IEEE 28th Intl. Parallel and Distributed Processing Symposium*. IEEE, 2014, pp. 349–359.
- [27] M. J. Bannister and D. Eppstein, “Randomized speedup of the Bellman–Ford Algorithm,” in *2012 Proc. of the Ninth Workshop on Analytic Algorithmics and Combinatorics (ANALCO)*. SIAM, 2012, pp. 41–47.
- [28] A. Weber, *Methoden zur Effizienzsteigerung abstraktionsbasierter Reglerentwurfverfahren*. München: Dr. Hut, 2018, Dissertation.
- [29] T. Kapela and P. Zgliczyński, “A Lohner-type algorithm for control systems and ordinary differential inclusions,” *Discrete Contin. Dyn. Syst. Ser. B*, vol. 11, no. 2, pp. 365–385, 2009.
- [30] A. Imdoukh, A. Shaker, A. Al-Toukhy, D. Kablaoui, and M. El-Abd, “Semi-autonomous indoor firefighting UAV,” in *2017 18th Intl. Conf. on Advanced Robotics (ICAR)*. IEEE, 2017, pp. 310–315.
- [31] H. Qin, J. Q. Cui, J. Li, Y. Bi, M. Lan, M. Shan, W. Liu, K. Wang, F. Lin, Y. Zhang *et al.*, “Design and implementation of an unmanned aerial vehicle for autonomous firefighting missions,” in *2016 12th IEEE Intl. Conf. on Control and Automation (ICCA)*. IEEE, 2016, pp. 62–67.
- [32] K. Harikumar, J. Senthilnath, and S. Sundaram, “Multi-UAV oxyrrhis marina-inspired search and dynamic formation control for forest firefighting,” *IEEE Trans. Automation Science and Eng.*, 2018.
- [33] W. Glover and J. Lygeros, “A stochastic hybrid model for air traffic control simulation,” in *Intl. Workshop on Hybrid Systems: Computation and Control*. Springer, 2004, pp. 372–386.
- [34] “Linux programmer’s manual,” <http://man7.org/linux/man-pages/man2/getrusage.2.html> accessed: 2019-09-01.